

Pulse propagation near highly reflective surfaces: Applications to photonic band-gap structures and the question of superluminal tunneling times

Michael Scalora, Jonathan P. Dowling, Aaron S. Manka, and Charles M. Bowden

Weapons Sciences Directorate, AMSMI-RD-WS-ST, U.S. Army Missile Command, Redstone Arsenal, Alabama 35898-5248

Joseph W. Haus

Physics Department, Rensselaer Polytechnic Institute, Troy, New York, 12180-3590

(Received 5 October 1994; revised manuscript received 1 February 1995)

We address the physics of pulse propagation, energy flow, and field dynamics as described by Maxwell's equations. After deriving the form of the Poynting vector for pulses that vary slowly in time only, we show that interference terms nontrivially affect the momentum and the energy density of an electromagnetic pulse that scatters from highly reflective materials. Inside such materials, we conclude that the magnetic- and electric-field amplitudes are strongly out of phase. We then apply our findings to the study of layered periodic structures; specifically, we examine the propagation of apparently "superluminal" pulses. By monitoring the local momentum and energy densities in the structure at all times, we explicitly show that the canonical energy velocity can never exceed the vacuum speed of light c at any point in the crystal.

PACS number(s): 42.50.Rh, 42.25.Bs, 42.25.Gy, 73.40.Gk

I. INTRODUCTION

The issues of propagation, energy flow, and field dynamics in electromagnetism have been of primary importance ever since the equations that describe these phenomena were first formulated in their entirety by Maxwell [1]. The validity of the theoretical predictions of Maxwell's equations rests on an overwhelming body of experimental evidence that has never been known to be in contradiction with the basic postulates of the theory, at least in the classical domain. These equations, therefore, form the basic underpinnings of all of modern optics, including nonlinear and quantum optics.

Although Maxwell's equations lay claim to all phenomena in classical optics, in practice many restrictive assumptions must be made in order to render the equations tractable. Chief among such approximations is the plane-wave limit that is typically applied in propagation problems. There is a danger, however, that the simplicity and omnipresence of the plane-wave approach can lead to a false sense of security and hence a tendency to overlook some of the more interesting physics that are involved in, say, pulse propagation or transverse effects. For instance, the study of propagating fields in nonlinear media in the plane-wave approximation overlooks interesting diffraction effects that become apparent only when the plane-wave limit is relaxed [2].

The study of two- and three-dimensional, periodic, dielectric structures—the so-called photonic band-gap (PBG) structures—has flourished in the past few years [3,4]. One-dimensional PBG structures have provided proof-of-principle results, and the prediction of new physical phenomena, such as band-gap solitons [5] and all optical switching [6]. In one dimension, these structures can be composed of alternating dielectric layers of different materials such that the index of refraction alter-

nates between a high and a low value, as in a quarter-wave-stack reflective coating. In three dimensions, a topologically complicated periodic index variation is required in order to obtain an omnidirectional band-gap structure [4]. The PBG crystal transmits a certain range of frequencies, while reflecting others. The name is applied in analogy to electronic semiconductor band gaps that arise in periodic crystal lattices in solid-state physics.

Recently, the dynamical characteristics of a pulse incident on a one-dimensional PBG material have been examined in the context of the numerical demonstration of a photonic band-edge laser [7], a nonlinear ultrafast optical limiter and switch [8], and a nonlinear optical diode [9]. In part, the work presented in this paper has been motivated by the recent controversy surrounding the definition and notion of a "tunneling time" associated with the speed at which an evanescent wave traverses a potential barrier [10]. A physically meaningful characterization of this time is desirable from a practical point of view in order to optimize high-speed, electronic nanostructures that utilize quantum tunneling, such as tunnel diodes. Chiao has pointed out that there are in fact several different characteristic velocities one may associate with an evanescent wave: the phase, group, energy, and front velocities [11]. In a series of experiments, Chiao and co-workers have measured the group velocity of single-photon wave packets traversing one-dimensional PBG structures. The photon frequency was chosen to correspond to the frequency at center gap, and although the tunneling appeared to be superluminal, they argued that it was a causal effect resulting from simple pulse reshaping [12]. Additional recent theoretical work by Chiao's group seems to indicate that in a linear gain medium, even the energy velocity can become superluminal [13].

With these considerations in mind, we will reexamine

the definition of energy velocity as it is usually applied to plane waves. In extending these considerations to pulses, we find some hitherto unknown features (to our knowledge) that form the major results of this paper. To begin, let us recall that the energy velocity V_e of a plane wave in a medium whose linear index profile is given by $n(z)$, where z is the direction of propagation, is usually defined as

$$V_e = \frac{|\mathbf{S}|}{U}, \quad (1)$$

where \mathbf{S} is the wave Poynting vector, and U is the local energy density of the electromagnetic field. However, this does not always agree with the wave group velocity, defined by

$$V_g = \frac{d\omega}{dk}. \quad (2)$$

In particular, V_e is a spatially local, time-dependent quantity, while V_g is not. These expressions are also commonly used to describe wave propagation in non-linear media. However, in regions of strong dispersion, different parts of the pulse may travel with quite different velocities, so much so that the assumption of a pulse with a well-defined peak moving in a single direction—used to derive V_g —breaks down. Under these circumstances, the time the wave packet takes to traverse a predetermined structure can be defined almost arbitrarily. From a physical standpoint, propagation in these structures is governed by Maxwell's equations, and one should then more properly refer to the Poynting vector as a natural measure of energy-transfer rates in any structure.

It is within the context of the discussion above that we undertake the study of the properties of electromagnetic pulses near highly reflective surfaces, starting only with Maxwell's equations. We will show that, even in the one-dimensional case, the magnetic and electric fields are not related in a simple way as they are for plane waves. In fact, interference terms affect the Poynting vector in a nontrivial fashion and also alter the usual notions of the momentum and the energy density of a traveling electromagnetic pulse. We will show that the magnetic field depends on the spatial curvature of the electric-field envelope and, near reflective surfaces, the two fields are spatially anticorrelated. In other words, where the electric field is a maximum, a minimum occurs in the magnetic field, and vice versa.

II. FORMALISM

We begin by writing the set of well-known Maxwell's equations. In Gaussian units, they are [14,15]

$$\nabla \cdot \mathbf{B} = 0, \quad (3)$$

$$\nabla \cdot \mathbf{D} = 4\pi\rho, \quad (4)$$

$$\nabla \times \mathbf{B} = \frac{4\pi}{c} \mathbf{J} + \frac{1}{c} \frac{\partial \mathbf{D}}{\partial t}, \quad (5)$$

$$\nabla \times \mathbf{E} = -\frac{1}{c} \frac{\partial \mathbf{B}}{\partial t}, \quad (6)$$

where for simplicity we have assumed that $\mathbf{B} = \mathbf{H}$, i.e., we deal with nonmagnetic materials for which $\mu = 1$. In addition, we make use of the constitutive relation

$$\mathbf{D} = \mathbf{E} + 4\pi\mathbf{P} = \epsilon\mathbf{E}. \quad (7)$$

Here, \mathbf{D} and \mathbf{P} are the electric-field displacement and volume polarization, respectively. The dielectric constant is ϵ , and it is related to the index of refraction by $\epsilon = n^2(z)$. Now we further assume that there are no free currents or charges, and that the electric and magnetic fields are linearly polarized. Then the fields are given by

$$\mathbf{E}(z, t) = \frac{1}{2} [E(z, t)e^{i(kz - \omega t)} + \text{c.c.}] \hat{\mathbf{x}}, \quad (8)$$

$$\mathbf{B}(z, t) = \frac{1}{2} [B(z, t)e^{i(kz - \omega t)} + \text{c.c.}] \hat{\mathbf{y}}, \quad (9)$$

where $E(z, t)$ and $B(z, t)$ are envelope functions, $\hat{\mathbf{x}}$ and $\hat{\mathbf{y}}$ are the usual x and y unit vectors, and $k = (\omega/c)n_0$ is assumed to be a constant initial value. Here n_0 is the real index of refraction of the background, or host medium, and it is assumed to be unity (i.e., the vacuum) without loss of generality. All phase-modulation effects that may result from propagation are, therefore, contained in the envelope functions. We neglect transverse effects and retain the longitudinal and temporal dynamics of the fields. We stress that Eqs. (8) and (9) for the fields merely constitute an initial condition, that is, the pulse is initially located in a host medium of uniform index $n_0 = 1$, and is traveling along the positive z direction.

A. Energy velocity for pulses

Substituting Eqs. (8) and (9) for the electric and magnetic fields into Maxwell Eq. (6), we immediately obtain

$$\frac{\partial E}{\partial z} + ikE = i\frac{\omega}{c}B - \frac{1}{c} \frac{\partial B}{\partial t}. \quad (10)$$

For pulses, this equation has an immediate solution for the magnetic field if we assume that the slowly varying envelope approximation in time holds (SVEAT), i.e.,

$$|\omega B| \gg \left| \frac{\partial B}{\partial t} \right|. \quad (11)$$

An expression similar to Eq. (11) holds for the electric field. The SVEAT implies that pulses should be at least 100 optical cycles long. Typical propagation distances do not exceed a full pulse width because structures can be extremely short. For example, if $\lambda = 1 \mu\text{m}$, a 100-optical cycle pulse can still be less than 1 ps, while a one-dimensional PBG crystal can be between 5 and 10 wavelengths long. As a result of the SVEAT, we can write Eq. (10) now as

$$B = E - i\frac{c}{\omega} \frac{\partial E}{\partial z}. \quad (12)$$

This simple result points to the important conclusion that the magnetic field is sensitive to the spatial modulation of the electric-field envelope. If the spatial modulation is small, i.e., if the pulse does not encounter a boundary, we may also neglect the spatial derivative term. Then $B \approx E$, which is the correct result in the plane-wave limit.

The important result here is that the spatial modulation of the electric field generates a phase shift in the magnetic field. This shift is dynamic and is significant when a field is incident on a highly reflective surface. Perhaps more importantly, this effect leads to a modification of the electromagnetic momentum and energy inside and, in general, near the surface of the structure. The Poynting vector is defined by [14,15]

$$\mathbf{S} = \frac{c}{4\pi} \mathbf{E} \times \mathbf{B}, \quad (13)$$

while the electromagnetic momentum density is given by [14]

$$\mathbf{g} = \frac{1}{4\pi c} \mathbf{E} \times \mathbf{B} = \frac{\mathbf{S}}{c^2}. \quad (14)$$

As a result, using the definition of the fields in Eqs. (8) and (9) above, and neglecting terms that oscillate at twice the optical frequency, we find that the electromagnetic momentum density is

$$g = \frac{1}{16\pi c} [EB^* + E^*B]. \quad (15)$$

Using Eq. (12), relating B to E and its spatial derivative, this expression becomes

$$\frac{S}{c^2} = g = \frac{1}{8\pi c} |E|^2 + \frac{i}{16\pi\omega} \left[E \frac{\partial E^*}{\partial z} - E^* \frac{\partial E}{\partial z} \right]. \quad (16)$$

Similarly, if the macroscopic medium [i.e., the absolute index of refraction $n(z)$] is assumed to be dispersionless and absorptionless over a finite range of frequencies, and strictly linear in both electric- and magnetic-field properties, the electromagnetic field energy density is given by [14,15]

$$U = \frac{1}{8\pi} (\mathbf{E} \cdot \mathbf{D} + \mathbf{B} \cdot \mathbf{B}). \quad (17)$$

Again using Eqs. (7)–(9) and (12), the energy density can be recast as

$$U = \frac{n^2(z)+1}{16\pi} |E|^2 + i \frac{c}{16\pi\omega} \left[E \frac{\partial E^*}{\partial z} - E^* \frac{\partial E}{\partial z} \right] + \frac{c^2}{16\pi\omega^2} \left| \frac{\partial E}{\partial z} \right|^2. \quad (18)$$

Our results suggest that the field envelope “curvature” resulting from interference effects can significantly alter the dynamical behavior of electromagnetic momentum and energy density near or inside a highly reflective struc-

ture such as a PBG material. In particular, the additional term present in the Poynting vector, from Eq. (16), containing factors of $\partial E/\partial z$ is reminiscent of the quantum-mechanical Schrödinger current density J in one dimension, given by [16]

$$J = \frac{i\hbar}{2m} \left[\Psi \frac{\partial \Psi^*}{\partial z} - \Psi^* \frac{\partial \Psi}{\partial z} \right], \quad (19)$$

where \hbar is Planck’s constant divided by 2π and m is the electronic mass. The similarity is striking and comes as a result of our reformulation in terms of slowly varying variables in time. In this case, the approximated Maxwell’s wave equation is first order in time and second order in space, in analogy to the Schrödinger equation.

The identification with the Schrödinger current should not be extended too far, and we merely point out that both wave equations are parabolic differential equations of the same type, and both lead to similar mathematical statements for energy and momentum conservation. In fact, the leading term on the right-hand side of Eq. (16) for the Poynting vector has no counterpart in Eq. (19). However, we stress here the new terms that appear in the Poynting vector, the momentum density and the energy density, are, to our knowledge, not normally taken into account. Their appearance strongly suggests the presence of *additional*, somewhat anomalous, local momentum and energy flow as a result of interference effects. Typically, the electromagnetic field is assumed to be nearly monochromatic, and the electric and magnetic fields are always in phase, even when the dispersion relation is quite complicated. We show below that these additional curvature effects can be quite dramatic when we consider pulse propagation inside a PBG structure, where a combination of velocity dispersion [17] (i.e., an implicit dependence of the effective index of refraction on frequency) and high reflectivity [7–9] yield complicated spatial field profiles. These profiles lead to significant phase shifts of the magnetic field with respect to the electric field.

One can see that if we wish to address momentum density, or total momentum in the electromagnetic field, the natural choice dictated by Maxwells’ equations is Eq. (16). On the other hand, the canonical energy velocity of light can also be derived from these quantities, as specified by Eq. (1). By using Eq. (16) for the Poynting vector and Eq. (18) for the energy density, Eq. (1) reduces to

$$V_e = c \frac{|E|^2 + i \frac{c}{2\omega} \left[E \frac{\partial E^*}{\partial z} - E^* \frac{\partial E}{\partial z} \right]}{\frac{n^2(z)+1}{2} |E|^2 + i \frac{c}{2\omega} \left[E \frac{\partial E^*}{\partial z} - E^* \frac{\partial E}{\partial z} \right] + \frac{c^2}{2\omega^2} \left| \frac{\partial E}{\partial z} \right|^2}. \quad (20)$$

We interpret this velocity to mean the speed at which electromagnetic energy is flowing locally, and it is a time- and position-dependent quantity. A brief examination shows that in the limit that the spatial variation of the index of refraction can be neglected, i.e., no boundaries are encountered and $\partial E/\partial z \approx 0$, the index of refraction $n(z)=1$ (the background index remains unmodulated), and the energy velocity is c , the speed of light in the medium. Further examination shows that the denominator of this expression can never be smaller than the numerator for real $n(z)$, leading to the conclusion that this expression for the energy velocity always yields a velocity less than or at most equal to the speed of light in the medium, in this case the vacuum.

B. Integrability of the energy density

Loudon has previously shown that an expression for the energy density, and consequently the energy velocity, can be derived in closed form for an incident plane-wave interacting with an oscillator medium [18]. Although Loudon's arguments and results were strictly model dependent, he found that the speed of light in an absorbing oscillator medium is subluminal. Chiao and co-workers have shown that in a gain medium modeled by harmonic oscillators far from resonance, in the steady-state limit, the imaginary part of the index of refraction can apparently lead to superluminal energy velocities for pulses [13]. However, we emphasize here that the basic assumption that we used to arrive at our expression for the energy density was that the medium was strictly linear and dispersionless, without any gain or loss [14,19]. If this is not the case, the general statement of energy conservation does not provide an explicit functional dependence of the energy density upon the fields. Other workers [19] also conclude that, in general, a simple expression for the energy density in terms of the fields can only be arrived at in the case of nondispersive propagation, a case that also includes the absence of absorption or gain. We now show this explicitly. Using energy conservation arguments, Maxwell's equations (3)–(6) lead to [14]

$$\int_V \mathbf{J} \cdot \mathbf{E} dV = -\frac{1}{4\pi} \int_V \left[c \nabla \cdot (\mathbf{E} \times \mathbf{H}) + \mathbf{E} \cdot \frac{\partial \mathbf{D}}{\partial t} + \mathbf{H} \cdot \frac{\partial \mathbf{B}}{\partial t} \right] dV. \quad (21)$$

The volume integral is over all space, and in the absence of free charges and currents, this expression can be recast as

$$\frac{\partial U}{\partial t} + \nabla \cdot \mathbf{S} = 0, \quad (22)$$

where the Poynting vector \mathbf{S} is given by Eq. (13), and

$$\frac{\partial U}{\partial t} = \frac{1}{4\pi} \left[\mathbf{E} \cdot \frac{\partial \mathbf{D}}{\partial t} + \mathbf{B} \cdot \frac{\partial \mathbf{H}}{\partial t} \right]. \quad (23)$$

As before, we assume no magnetic effects in the material, and take $\mathbf{B}=\mathbf{H}$. Equation (22) above guarantees total en-

ergy conservation. Now, using the definitions of Eqs. (8) and (9) for the electric and magnetic fields, and assuming that the polarization can also be written in similar form, Eq. (23) becomes

$$\frac{\partial U}{\partial t} = \frac{1}{16\pi} \frac{\partial}{\partial t} (|E|^2 + |B|^2) + \frac{1}{4} \left[E \frac{\partial P^*}{\partial t} + E^* \frac{\partial P}{\partial t} \right] + i \frac{\omega}{4} (EP^* - E^*P), \quad (24)$$

where P is the polarization envelope function. Each of the terms on the right-hand side of Eq. (24) can be given its own physical meaning. The first term is clearly the rate of change of the energy present in the field. The second and third terms are a measure of the energy exchanged between the electric field and the bound current density. Hence, these terms include the work done by the field on the bound charges, as well as the rate at which energy is transferred to and from the medium.

One can see that, in general, a simple expression for U , the energy density, cannot be easily arrived at unless the medium response is linear. If, for example, $\mathbf{P}=[(n^2-1)/4\pi]\mathbf{E}$ as in Eq. (7), and n is purely real and time independent, Eq. (17) can be recovered from Eq. (24). However, if n is complex and of the form $n=n_r+i n_i$, where n_i can be positive or negative, linear gain or loss is possible. It is then easy to verify that Eq. (24) becomes

$$\frac{\partial U}{\partial t} = \frac{1}{16\pi} \frac{\partial}{\partial t} \left[(n_r^2 - n_i^2) |E|^2 + |B|^2 \right] + \frac{2in_r n_i}{16\pi} \left[E^* \frac{\partial E}{\partial t} - E \frac{\partial E^*}{\partial t} \right] + \frac{4\omega n_r n_i}{16\pi} |E|^2. \quad (25)$$

A closed-form integration for the energy density cannot be obtained from this expression unless the field in the medium is known *a priori*. In any case, the fact that Eqs. (24) and (25) cannot in general be further simplified prevents us from reaching any definite conclusion as to the value of the energy velocity V_e . In other words, substituting the plane-wave results for S and U into the definition of V_e , Eq. (1), may lead to incorrect results for a linear gain medium because, as we have seen, it is nearly impossible to produce a self-consistent expression for the time-integrated energy density U from Eq. (25). Hence we caution that the interpretation of a superluminal energy velocity in a linear gain medium material depends crucially on how the energy density is defined. The plane-wave approximation for S and U may yield answers that are perhaps too simplistic or misleading.

Another case of interest that does allow the derivation of an explicit form of the energy density U is the interaction of ultrashort pulses with a dilute set of two-level atoms. The equations of motion that describe the dynamics are known as the optical Bloch equations, and they can be written as [20]

$$\frac{\partial W}{\partial t} = \frac{2\mu i}{\hbar} (ER^* - E^*R), \quad (26)$$

$$\frac{\partial R}{\partial t} = i\delta R - i\frac{\mu}{\hbar} EW, \quad (27)$$

where W and $P = 2N\mu R$ are the medium inversion and polarization, respectively, N is the atomic density, μ is the atomic dipole moment, and $\delta = \omega - \omega_0$. Here, ω_0 is the two-level atom frequency spacing, and δ is, therefore, a small detuning from resonance. Equation (26) represents the rate at which atoms are excited, while Eq. (27) gives the dynamics of the complex nonlinear index of refraction. Notice that all relaxation rates have been neglected because we assume extremely short interaction times. In this case, using Eqs. (26) and (27), Eq. (24) can be integrated directly, unlike the previous example with a linear gain material. The electromagnetic energy density reduces to

$$U = \frac{1}{16\pi} (|E|^2 + |B|^2) + \frac{N\hbar\omega_0}{4} (W + 1). \quad (28)$$

The factor $(W + 1)$ follows from the definition of the ground state at $W = -1$ [20]. Again, we emphasize that both energy density and the Poynting vector are local, time-dependent quantities. Although the second term is proportional to ω_0 regardless of detuning, the temporal evolution of the inversion preserves information about detuning via the dynamics of Eqs. (26) and (27). Upon neglecting reflections, i.e., $n(z) = 1$, $\partial E / \partial z \ll kE$, and $B \approx E$, the electromagnetic energy velocity is given by

$$V_e = \frac{c}{1 + \frac{2\pi N\hbar\omega_0 (W + 1)}{|E|^2}}. \quad (29)$$

Clearly, this velocity is intensity dependent, although, as we pointed out, the inversion retains an implicit dependence on detuning, time, and field amplitude as well. Nevertheless, from Eq. (29) one can conclude that the energy velocity V_e is *always* smaller than c , regardless of the state of excitation of the medium. Although we will not dwell on this point here, it is interesting to note that the limit $V_e = c$ is obtained when the medium is in the ground state (for small field values $W = -1$) and for very high intensities, while V_e is a minimum when the medium is completely excited ($W = 1$).

To conclude this section, we point out that, in general, Eq. (21) suggests that the Poynting vector and momentum density remain unaffected for nonlinear media. Although some controversy still remains about the actual form of the momentum density, most workers agree on the definition of Eq. (14). The alternative definition, due to Minkowski, uses \mathbf{D} instead of \mathbf{E} , and can sometimes also be found in the literature [21]. However, the Minkowski form is often viewed as unacceptable because it yields a stress-energy tensor that lacks symmetry [14].

III. EXAMPLE: PHOTONIC BAND-GAP STRUCTURES

In order to illustrate some of the results presented in the previous sections, we consider pulse propagation inside a PBG structure. We consider a multilayer stack of dielectric material that is arranged in such a way that alternating layers have a high index of refraction n_2 , and a low n_1 . The thickness of each layer also alternates and is such that $a = \lambda / (4n_1)$ and $b = \lambda / (4n_2)$, where λ is the

free-space wavelength. This dielectric stack forms a reflective dielectric coating, and it is usually referred to as a distributed Bragg reflector. For normally incident light, a range of wavelengths centered about λ_{cg} , the wavelength at center gap will be reflected, that is, propagation of those wavelengths is not allowed inside the structure and only evanescently decreasing or tunneling modes are allowed.

A. Numerical model for pulse propagation in PBG structures

We use a numerical model to solve for the dynamics of the fields [7–9,22]. We assume that the field propagates in the z direction, it is paraxial, and that it separates into an envelope function that varies slowly in time, and a rapidly oscillating factor, as per Eq. (8). Upon direct substitution, Maxwell's equation for the propagation of an electric field in a one-dimensional photonic band-gap material can be written in dimensionless form as

$$\frac{\omega_{cg}}{\omega} \frac{\partial^2 E}{\partial \xi^2} + 4\pi i \frac{\partial E}{\partial \xi} + 4\pi i \frac{\partial E}{\partial \tau} = -\frac{4\pi^2 \omega}{\omega_{cg}} [n^2(\xi) - 1] E. \quad (30)$$

Here, $\xi = z / \lambda_{cg}$ is the longitudinal coordinate scaled by the wavelength at center gap, ω_{cg} is the corresponding center gap frequency, $\tau = ct / \lambda_{cg}$ is the time scaled by the corresponding optical period, and $n(\xi)$ is the refractive index of the medium that contains information regarding the linear response of the structure. We neglect any nonlinear effects, and choose λ to be the carrier wavelength. Equation (30) for the electric field is supplemented by Eq. (12), the copropagating magnetic field B . In dimensionless form, Eq. (12) above can be rewritten as

$$B = E - \frac{i}{2\pi} \frac{\partial E}{\partial \xi}. \quad (31)$$

For simplicity, the field envelope E is assumed to have a Gaussian profile that is initially located outside the structure traveling with group (or phase) velocity c . Its width when the amplitude is $1/e$ of its peak values is taken to be nearly 160 optical cycles, thus ensuring that the slowly varying envelope approximation in time is well satisfied. The linear index profile for the Bragg reflector is depicted in Fig. 1.

We now discuss our results. We choose $n_1 = 1$, and $n_2 = 1.41$, a total of 39 layers, and tune the incoming pulse so that its carrier frequency is in the photonic pass band, but near the band edge at the low-frequency side of the quarter-wave band gap, so that $\omega / \omega_{cg} = 0.885$, and nearly 50% of the pulse is transmitted [7–9]. This transmission (or reflection) is due to the fact that the pulse contains a finite spread of frequencies. Tuning the carrier frequency near the band edge causes some frequencies to be reflected more than others, resulting, in this case, in nearly one half of the energy being transmitted.

In Fig. 2, we plot the $|E|^2$ profile obtained through direct integration of the E propagation Eq. (30) (solid line), and the accompanying magnetic field obtained using the auxiliary Eq. (31) (dotted line). This plot shows

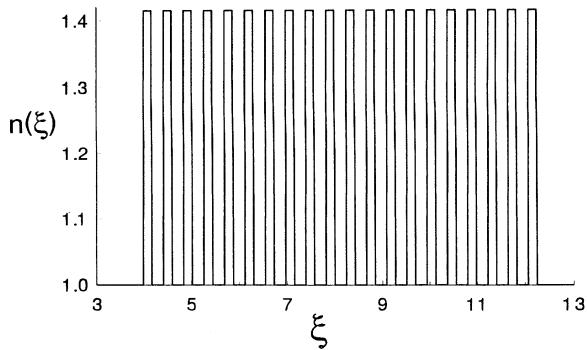


FIG. 1. Typical one-dimensional photonic band-gap crystal. It consists of alternating dielectric layers of high and low index of refraction. In this case, $n_1=1$, and $n_2=1.41$. The width of each layer is chosen to be about one quarter of the local value of the wavelength. The longitudinal coordinate ξ is given in units of the wavelength at center gap, λ_{cg} .

the field eigenmodes, and it corresponds to a moment when the pulse is interacting strongly with the structure. The effective index profile is also depicted in the figure. The figure shows that the fields are strongly out of phase (nearly $\pi/2$) inside the structure, and that a local maximum (or minimum) of the electric field corresponds to a zero of the magnetic field. Under the circumstances described at the end of the preceding paragraph, effective transmission ($\geq 90\%$) cannot occur since locally $\mathbf{E} \times \mathbf{B}$ —and hence \mathbf{S} —is small, and the fields nearly become standing waves. We point out that in order to have effective transmission, both fields should always be in

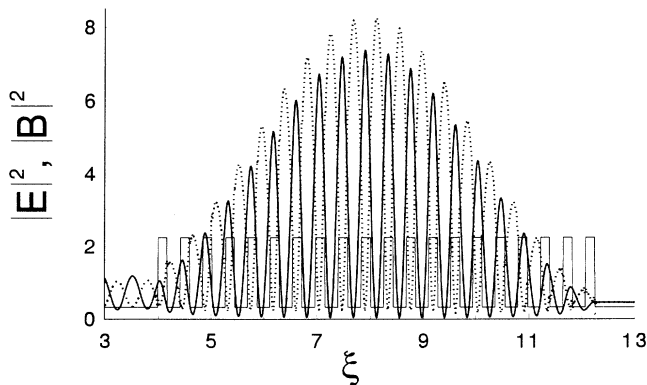


FIG. 2. Electric- (solid line) and magnetic-field (dotted line) profiles inside and near the PBG crystal (solid line, not to scale), as a function of position inside the crystal. The coordinate ξ is scaled as in Fig. 1. The pulse is incident from the left, and its $1/e$ width is nearly 160 optical cycles, and $\omega/\omega_{cg}=0.885$. Inside and to the left of the structure, the fields are spatially strongly anticorrelated. Far and to the right of the structures, the fields are in phase and overlap because the interference of left- and right-propagating waves either subsides (far from the PBG), or does not occur (everywhere to the right of the PBG).

phase, although some overlap of the field wave packets can also lead to significant transmission, as in this case. We emphasize that while the magnitude of the Poynting vector does not vary drastically as a function of frequency near the band edge, it may actually become several orders of magnitude smaller and nonoscillatory for a pulse tuned near the center of the gap. That it does not oscillate and its magnitude is greatly reduced inside the gap should be expected; this is in fact an indication that evanescently decaying modes are excited inside the structure, and that no eigenmodes are supported by the structure at those frequencies.

An analogous circumstance occurs in metals or good conductors [15], where the fields undergo a quadrature phase shift similar to what we have reported above, and nearly complete reflection occurs. In that case, however, the large phase shift between the fields comes about because the propagation vector is complex [15]. We point out that near the band edge of the PBG crystal, the fields are also nearly standing waves, leading to large reflections. We note that far enough away from the structure the condition $B=E$ is well satisfied, and the fields are in phase and overlap.

B. Midgap pulse tunneling

We now address the question of electromagnetic momentum and the apparent superluminal behavior associated with the group velocity of pulses propagating through PBG structures [11]. We calculate the momentum density using Eqs. (12) and (15). Let us consider a PBG structure with a total of 14 layers, and we tune the incoming pulse in the center of the gap, as was done under experimental conditions by Chiao and co-workers [11,12]. Actually, this structure does not have a true gap in the sense that the minimum transmission at gap center is greater than 5%. This can be seen in Fig. 3, where we plot the input and the scattered electromagnetic momentum density of the pulse as a function of the longitudinal coordinate. Note that the reflected pulse acquires negative momentum (the pulse undergoes a π flip upon

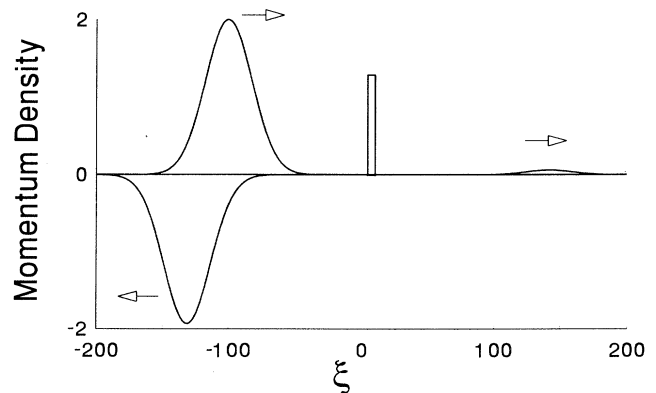


FIG. 3. Incident and scattered electromagnetic momentum density as a function of position for a pulse tuned to the frequency at center gap ($\omega/\omega_{cg}=1$) of a 14-layer structure. The initial pulse is that of Fig. 2, and ξ is in units of the wavelength at center gap. Note the sign change for the momentum of the reflected pulse.

reflection), and that the total momentum is not conserved; this is due to the fact that we assume that the structure has infinite mass, and so it acts like a “source” of momentum.

In Fig. 4, we compare the transmitted pulse of Fig. 3 with a pulse that propagates in vacuum. The figure shows that for similar propagation times, the amplitude of the leading edge of the pulse that propagates in free space is much *larger* than the leading edge of the pulse that propagates through the structure. Now at least some part of the tunneling pulse would have to be in front in order to achieve superluminal behavior. However, no part of the tunneling pulse ever crosses or leads the freely propagating pulse, and propagation therefore remains causal at all times. The inset of Fig. 4, however, shows the fields normalized to unity. Here, the *peak* of the pulse that propagates in vacuum lags behind the *peak* of the tunneling pulse by several optical wavelengths. The lag time depends on the number of layers, and in this case, the lag time increases (i.e., larger forward shifts occur) with the addition of more layers. The process of adding more layers, however, increases the depth and sharpens the width of the band gap, reducing the transmitted peak intensity, along with the transmitted energy, by several more orders of magnitude. Numerically, the transmission becomes essentially zero ($\leq 10^{-4}$) when the total number of layers is over 20. Our calculations confirm that while the energy velocity V_e of Eq. (20) can change quite rapidly between layers, we find that it *always* remains smaller than the vacuum value. The observed forward shift of the peak of the pulse can then be understood only as a reshaping of the wave packet, and not as an effect due to superluminal energy velocity components. This fact was recently pointed out by Chiao and co-workers [11], and here we have explicitly shown how

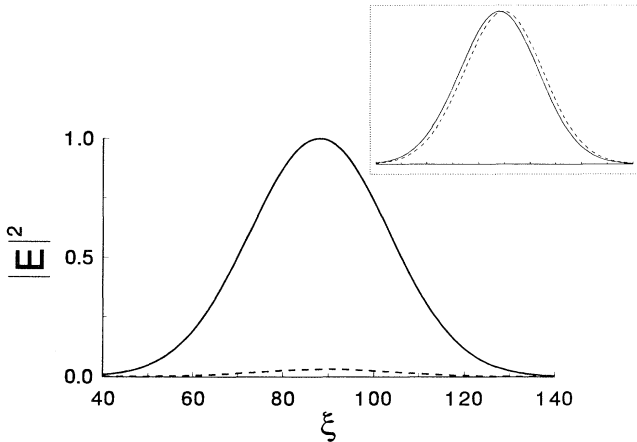


FIG. 4. Spatial distribution of the transmitted $|E|^2$ profiles for a pulse that propagates in free space (solid line), and for a pulse tuned at the midgap frequency that tunnels through a structure that is located at the origin (dashed line). The parameters and units are those of Figs. 2 and 3. The amplitude of the tunneling pulse is everywhere much smaller than the amplitude of the pulse that propagates in free space. Because the fields never cross, the tunneling pulse can never lead, and propagation is causal.

this works with both the derivation of Eq. (20), and with a numerical simulation.

C. Pulse propagation at band-edge frequencies

For completeness, we point out that we have also investigated velocity distributions for other pulses with frequencies near the band edge, (as opposed to gap center) and different pulse shapes, such as a hyperbolic secant, and broader Gaussian functions. All of them gave results consistent with what we have reported above, that is, the local energy velocity never exceeds the velocity of light in a vacuum in a linear system without gain or loss. In addition, the transmitted pulse appears to retain its original shape only if the incident pulse is tuned near the frequency at center gap. This was reported in the Berkeley experiment of Ref. [12] (this point is discussed in Ref. [13] and references therein), and held true in our numerical simulations for the various pulse shape we investigated. Although the actual energy and momentum densities may exceed vacuum levels manyfold for pulses with a control frequency near the band edge, this is an effect that comes as a result of increased Bragg scattering. A decrease in group velocity takes place, hence a slow down of the pulse occurs. This, in turn, increases photon density, which translates to an increase in both momentum and energy densities inside the crystal. The transmitted pulse then clearly lags behind the pulse that propagates in free space, as shown in Fig. 5. In this case, while the incident pulse is Gaussian in shape, the transmitted wave packet is not. This implies that the large velocity dispersion that occurs at the band edge, coupled to the larger interaction time, is enough to induce changes in pulse shape. This does not happen for the pulse tuned at center gap because the transmission is nearly the same for all frequencies within the pulse, which in turn hardly experiences any dispersion.

D. A new measure of tunneling time

Finally, we address the question of tunneling time. From our point of view, the interaction time of a pulse

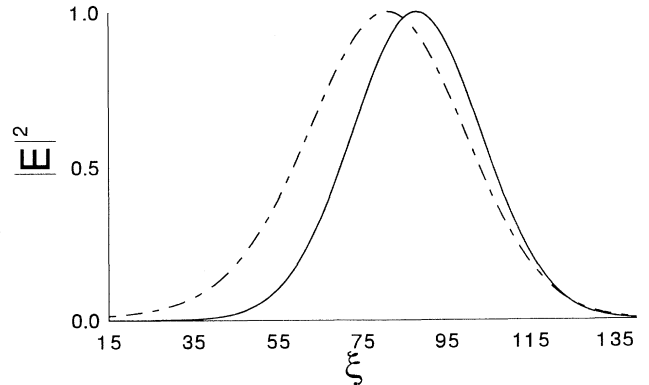


FIG. 5. Comparison between a pulse that propagates in free space (solid line), and a pulse tuned near the band edge of the structure of Fig. 1 (dashed line). Parameters and units are the same as those of Fig. 2.

with an arbitrary structure must be nonzero and cannot be retrieved from a steady-state wave-function distribution such as an exponential evanescent wave [10] because this tunneling description process explicitly neglects the dynamical development of the system. Although a satisfactory definition of a tunneling time still remains elusive, we would like to propose a definition of the tunneling time simply as the time the pulse spends inside the structure. Recently, Støvneng has explicitly shown that this time is actually the only physically meaningful representation of a tunneling time [23].

We now use our numerical model to calculate the pulse dwell time inside the structure. We monitor the total spatially integrated energy within the crystal as a function of time, and compare the three cases we have investigated above, namely, free-space propagation, propagation at gap center, and propagation near the band edge. We do not resort to invoking the concept of group velocity because, while it can be defined near the band edge, at center gap it becomes analytically ambiguous [7,10–13]. Instead, we simply allow the pulse to propagate through the crystal, and measure energy buildup time for these three separate cases. We first begin with a pulse that propagates in free space, which we will use as our “stopwatch” to time the others. Because the length of the interval is much smaller than the pulse width, the interaction time is then roughly equivalent to the duration of the pulse. This interaction time is to be distinguished from the transit time, which may be very different for different pulse widths. In Fig. 6, curve *a*, we plot the total energy as a function of time within the specified interval for a pulse propagating in vacuum. Curve *b* in the figure is the total energy in the structure as a function of time for a pulse tuned near the band edge, and the parameters used are those of Fig. 2. The delay that is ap-

parent between the two curves is due to the low group velocity that the pulse acquires when tuned near the band edge. In other words, the pulse peak is shifted backward in time, as expected. The fact that the width of the band-edge energy curve is much broader indicates a long dwell time, in concert with a small group velocity and effective dispersion.

Finally, curve *c* represents the total energy as a function of time for a pulse tuned at center gap, where tunneling occurs. This energy curve is for the pulse of Fig. 4, whose physical peak is shifted forward in space by several optical periods when compared to free-space propagation. Accordingly, here we find this energy curve peak is shifted forward in time, i.e., shifted to the left. However, we stress that the widths of the free-space propagation energy curve *a* and the curve that evolves at center gap *c* are essentially the same to within one tenth of an optical cycle, except for the small peak-to-peak time shift. That is, the interaction times depicted in Fig. 6 for curves *a* and *c* are the same to approximately one part in one thousand. This difference is insignificant, if taken within the context of the SVEAT approximation.

If we now combine the results of our numerical “experiment” of the previous sections, with our analytical results, which show that the local energy velocity remains subluminal inside the structure, Eq. (20), then the interaction or dwell time of a tunneling pulse appears to be the same as that of a pulse propagating in free space. From a physical standpoint, the fact that the energy velocity, Eq. (20), does not exceed the vacuum velocity *c* was expected. What is perhaps more remarkable, as well as surprising, is the fact that a pulse that propagates in matter may in fact tunnel through the structure as if it were propagating in free space—an event to which some theories ascribe infinite speed [10]. The pulse is essentially trying to do the best it can to achieve this as it propagates through the structure, and our conclusion, based on both our numerical and analytical results, is that the transfer of energy through the structure occurs at the rate at which energy would be transferred in vacuum, in full accord with Einstein’s causality. Again we have tested this result for several pulse shapes, and different values of the refractive indices, and we reach the same conclusion.

This conclusion does not in any way contradict our finding that the peak of the pulse that propagates at the center gap frequency is shifted forward in time when compared to free-space propagation. The reshaping of the wave packet only assigns an apparent superluminality to the *probability of detection* of a photon; however, to date no information can be transmitted in this fashion by any known process. The probability of detection has nothing to do with the implication of our results, which are: (1) For linear systems, electromagnetic energy cannot be transmitted locally or globally at speeds higher than *c*, and (2) a pulse tuned at the midgap frequency propagates with a tunneling velocity at or near the vacuum velocity of light.

IV. CONCLUSION

In conclusion, we have shown that pulse dynamics near and inside highly reflective structures can be quite com-

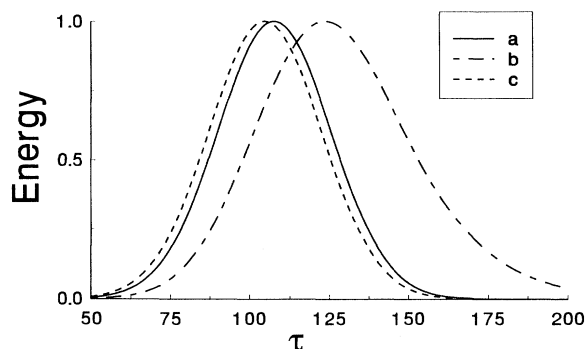


FIG. 6. Total energy as a function of time within a specified volume for the three cases we have discussed, that is, for the case of a pulse that propagates in free space (curve *a*, solid line), the case of propagation at the band edge (curve *b*, dashes of alternating length), and the case of a pulse tuned at center gap (curve *c*, short dashes). The time is scaled in units of the optical period that corresponds to the wavelength at center gap. Our control parameters are provided by the pulse that propagates in free space. The width of these curves corresponds to the pulse dwell time inside the PBG structure.

plicated leading to a nontrivial relationship between the electric- and magnetic-field envelopes. A significant phase shift arises in the magnetic field as a result of a strong spatial modulation of the electric field, leading in the SVEAT to an auxiliary curvature equation for the magnetic field, Eq. (12). This constraint on the form of B yields an equation in E for energy flow that is similar in form to the Schrödinger current. These curvature effects can dominate when there is a strong spatial modulation of the electric-field envelope, as there is near highly reflective surfaces, or in photonic band-gap structures. The spatial decoupling that occurs between the electric and magnetic fields can be important in isolating and studying either electric or magnetic effects independently. Field dynamics are driven by frequency filtering, velocity dispersion [17], and interference effects that are especially strong near the band edge. These effects may lead to a reshaping and a forward shift of the wave packet as it tunnels through the PBG structure, as observed in experiments [12]. However, we have shown that the velocity distribution of the pulse does not exceed the velocity of light in vacuum, and that the minimum time necessary for the field-matter interaction to occur is not smaller than the free-space propagation interaction time.

It appears then, from our dwell-time simulations and the analytical results of Eq. (20), that the tunneling of a pulse through a linear photonic band-gap material takes place at a speed at, or nearly equal to, the vacuum velocity of light. It is gratifying to find that it is no faster than this—but somewhat remarkable that it does not appear to be slower than this, considering that the pulse propagates through matter. We have also shown that, in gen-

eral, for nonlinear or dispersive systems an explicit expression for the energy density U cannot be obtained, and the form of Eq. (24) precludes us from reaching any *a priori* definite conclusions about the energy velocity of light in such materials, since the V_e of Eq. (1) cannot be solved for in closed form. To date, the dynamical characteristics of the system remain poorly understood. Because of its very fundamental nature, this problem will remain an interesting one, and promises to remain fertile ground for many future investigations.

Finally, we point out that the derivation of Eq. (20) for the canonical energy velocity of a pulse can trivially be extended to three dimensions. However, because the vector qualities of the electromagnetic field must then be retained in the numerical simulations as well, the pulse propagation algorithm that we have used [7–9,22] must be appropriately modified.

ACKNOWLEDGMENTS

The authors would like to thank F. Todaro, R. Y. Chiao, H. O. Everitt, P. G. Kwiat, M. J. Bloemer, A. M. Steinberg, P. M. Steinberg, and M. Tocci, for interesting and valuable discussions related to this work. M. S. acknowledges support by ARO Grant No. DAAH-04-93-D-0002. M. S. and J. P. D. acknowledge support by Battelle Scientific Services Agreement No. DAAL03-91-C-0034. M. S., J. P. D., and A. S. M. acknowledge partial financial support from the National Research Council. J. W. H. acknowledges support by ARO Grant No. 31051-PH, and NSF Grant No. ECS-9301075.

-
- [1] J. C. Maxwell, *Treatise on Electricity and Magnetism*, 3rd ed. (Dover, New York, 1954).
 - [2] J. V. Moloney, M. R. Belic, and H. M. Gibbs, *Opt. Commun.* **41**, 379 (1982); F. P. Mattar and C. M. Bowden, *Phys. Rev. A* **27**, 345 (1983); J. W. Haus and M. Scalora, *ibid.* **42**, 3149 (1990); M. Scalora and J. W. Haus, *J. Opt. Soc. Am. B* **5**, 1003 (1991).
 - [3] E. Yablonovitch, *Phys. Rev. Lett.* **58**, 2169 (1987).
 - [4] *Development and Applications of Photonic Band Gap Materials*, edited by C. M. Bowden, J. P. Dowling, and H. O. Everitt, special issue of *J. Opt. Soc. Am. B* **10**, 279 (1993); *J. Mod. Opt.* **41**, 171 (1994), special issue on photonic band-gap structures, edited by G. Kurizki and J. W. Haus.
 - [5] W. Chen and D. L. Mills, *Phys. Rev. Lett.* **58**, 160 (1987); C. M. de Sterke and J. E. Sipe, *Phys. Rev. A* **38**, 5149 (1988); *ibid.* **39**, 5163 (1989).
 - [6] N. D. Sankay, D. F. Prelewitz, and T. G. Brown, *Appl. Phys. Lett.* **60**, 1427 (1992).
 - [7] J. P. Dowling, M. Scalora, M. J. Bloemer, and C. M. Bowden, *J. Appl. Phys.* **75**, 1896 (1994).
 - [8] M. Scalora, J. P. Dowling, C. M. Bowden, and M. J. Bloemer, *Phys. Rev. Lett.* **73**, 1368 (1994).
 - [9] M. Scalora, J. P. Dowling, C. M. Bowden, and M. J. Bloemer, *J. Appl. Phys.* **76**, (1994).
 - [10] M. Büttiker and R. Landauer, *Phys. Rev. Lett.* **49**, 1739 (1982); E. H. Hauge and J. A. Støvneng, *Rev. Mod. Phys.* **61**, 917 (1989); H. A. Fertig, *Phys. Rev. Lett.* **65**, 2321 (1990).
 - [11] R. Y. Chiao, *Quantum Opt.* **6**, 359 (1994).
 - [12] R. Chiao, P. G. Kwiat, and A. M. Steinberg, *Physica B* **175**, 257 (1991); A. M. Steinberg, P. G. Kwiat, and R. Y. Chiao, *Phys. Rev. Lett.* **71**, 708 (1993).
 - [13] R. Y. Chiao, *Phys. Rev. A* **48**, 34 (1993); E. L. Bolda, R. Y. Chiao, and J. C. Garrison, *ibid.* **49**, 2938 (1994).
 - [14] J. D. Jackson, *Classical Electrodynamics*, 2nd ed. (Wiley, New York, 1975), Chap. 6.
 - [15] J. B. Marion, *Classical Electromagnetic Radiation*, 1st ed. (Academic, London, 1965), Chap. 6.
 - [16] L. I. Schiff, *Quantum Mechanics*, 3rd ed. (McGraw Hill, New York, 1968), p. 26.
 - [17] J. P. Dowling and C. M. Bowden, *J. Mod. Opt.* **41**, 345 (1994).
 - [18] R. Loudon, *J. Phys. A* **3**, 233 (1970).
 - [19] L. D. Landau and E. M. Lifshitz, *Electrodynamics of Continuous Media*, 2nd ed. (Pergamon, New York, 1984), Chaps. 9 and 10.
 - [20] L. Allen and J. H. Eberly, *Optical Resonance and Two-Level Atoms*, 1st ed. (Wiley, New York, 1975), Chap. 4 (republished by Dover, New York, 1987).
 - [21] F. S. Johnson, B. L. Cragin, and R. R. Hodges, *Am. J. Phys.* **62**, 33 (1994).
 - [22] M. Scalora, *J. Opt. Soc. Am. B* **11**, 770 (1994); M. Scalora and M. E. Crenshaw, *Opt. Commun.* **108**, 191 (1994).
 - [23] J. A. Støvneng, *25th Winter International Workshop on Quantum Electronics, Snowbird, Utah, 1995* (unpublished).